OAK RIDGE NATIONAL LABORATORY LIBRARY

3 4456 0022299 8

ORNL/TM-5907

Cy. 1

Automatic Particle-Size Analysis of HTGR Recycle Fuel

J. E. Mack
W. H. Pechin

OAK RIDGE NATIONAL LABORATORY
CENTRAL RESEARCH LIBRARY
DOCUMENT COLLECTION
LIBRARY LOAN COPY
DO NOT TRANSFER TO ANOTHER PERSON
If you wish someone else to see this document, send in name with document and the library will arrange a loan.

UCN-7969
(3 3-67)

OAK RIDGE NATIONAL LABORATORY
OPERATED BY UNION CARBIDE CORPORATION FOR THE ENERGY RESEARCH AND DEVELOPMENT ADMINISTRATION

Printed in the United States of America. Available from
National Technical Information Service
U.S. Department of Commerce
5285 Port Royal Road, Springfield, Virginia 22161
Price: Printed Copy $4.00; Microfiche $3.00

This report was prepared as an account of work sponsored by the United States Government. Neither the United States nor the Energy Research and Development Administration/United States Nuclear Regulatory Commission, nor any of their employees, nor any of their contractors, subcontractors, or their employees, makes any warranty, express or implied, or assumes any liability or responsibility for the accuracy, completeness or usefulness of any information, apparatus, product or process disclosed, or represents that its use would not infringe privately owned rights.

ORNL/TM-5907
Distribution
Category UC-77

Contract No. W-7405-eng-26

OAK RIDGE NATIONAL LABORATORY
GAS-COOLED REACTOR PROGRAMS

Thorium Utilization Program
(189a OHO45)

Fuel Refabrication – Task 300

AUTOMATIC PARTICLE-SIZE ANALYSIS OF HTGR RECYCLE FUEL

J. E. Mack and W. H. Pechin

Date Published: September 1977

OAK RIDGE NATIONAL LABORATORY
Oak Ridge, Tennessee 37830
operated by
Union Carbide Corporation
for the
Energy Research and Development Administration

OAK RIDGE NATIONAL LABORATORY LIBRARY
3 4456 0022299 8

AUTOMATIC PARTICLE-SIZE ANALYSIS OF HTGR RECYCLE FUEL

J. E. Mack and W. H. Pechin

ABSTRACT

An automatic particle-size analyzer was designed, fabricated, tested, and put into operation measuring and counting HTGR recycle fuel particles. The particle-size analyzer can be used for particles in all stages of fabrication, from the loaded, uncarbonized weak acid resin up to fully-coated Biso or Triso particles. The device handles microspheres in the range of 300 to 1000 μm at rates up to 2000 per minute, measuring the diameter of each particle to determine the size distribution of the sample, and simultaneously determining the total number of particles.

INTRODUCTION

The High-Temperature Gas-Cooled Reactor (HTGR)[1,2] is one of the promising reactor concepts being developed at this time. It offers high thermal efficiency and conserves uranium by using thorium for a portion of its fuel. The high reactor temperatures are possible because graphite is used as both moderator and core structure and because pyrolytic carbon and silicon carbide coatings surround the fuel to retain fission products. The need for metal cladding is thus eliminated. Figure 1 illustrates the two fuel particle types (fissile and fertile) along with the fuel rod and hexagonal graphite core element.

The reactor fuel consists of small spherical uranium oxide–uranium carbide fissile and thorium oxide fertile coated particles. The bare particles or "kernels" are coated with various layers of pyrolytic carbon and silicon carbide. Fissile particles are of the "Triso" design;[3] they receive three types of coatings, as illustrated in Fig. 2. The fertile particles are of the "Biso" design; they receive only two coatings. Each layer is designed for a specific purpose and must have certain specified properties. The innermost or buffer coating for both Triso and Biso particles is composed of low-density pyrolytic carbon. The buffer provides void space for the accumulation of fission products and serves to shield other layers from damage by fission fragment recoils. The next layer in both the Triso and Biso particle types is known as a low-temperature isotropic layer (LTI): the carbon layer is deposited at a low temperature as compared to certain other processes, and the carbon must be crystallographically isotropic to avoid excessive shrinkage caused by radiation during service. The LTI layer has a higher density than the buffer layer and it acts as a pressure vessel to contain gaseous fission products. This is the last coating applied to the fertile particle and, as is the case with the buffer coating, the layer is considerably thicker in the Biso than in the Triso design. The third coating applied to the fissile particle is composed of high-density silicon carbide which acts as a diffusion barrier to metallic fission products. The fissile particle also has an outer coating of low-temperature isotropic pyrolytic carbon (OLTI) which enhances the bonding which occurs when the fuel particles are formed into rods with a carbonaceous matrix.

---

1. H. B. Stewart, R. C. Dahlbert, W. V. Goeddel, D. B. Trauger, P. R. Kasten, and A. L. Lotts, "Utilization of the Thorium Cycle in the HTGR," pp. 433–47 in *Peaceful Uses of Atomic Energy, Proc. 4th Int. Conf., Geneva, 1971,* vol. 4, United Nations, New York and International Atomic Energy Agency, Vienna, 1972.

2. Oak Ridge National Laboratory, Gulf General Atomic, and Idaho Chemical Processing Plant, *National HTGR Fuel Recycle Development Program Plan,* ORNL-4702, Rev. 1 (Draft, Aug. 11, 1973).

3. W. O. Harms, "Carbon Coated Carbide Particles for Nuclear Fuels," pp. 290–313 in *Modern Ceramics – Some Principles and Concepts,* ed. by J. E. Hove and W. C. Riley, Wiley, New York, 1965.

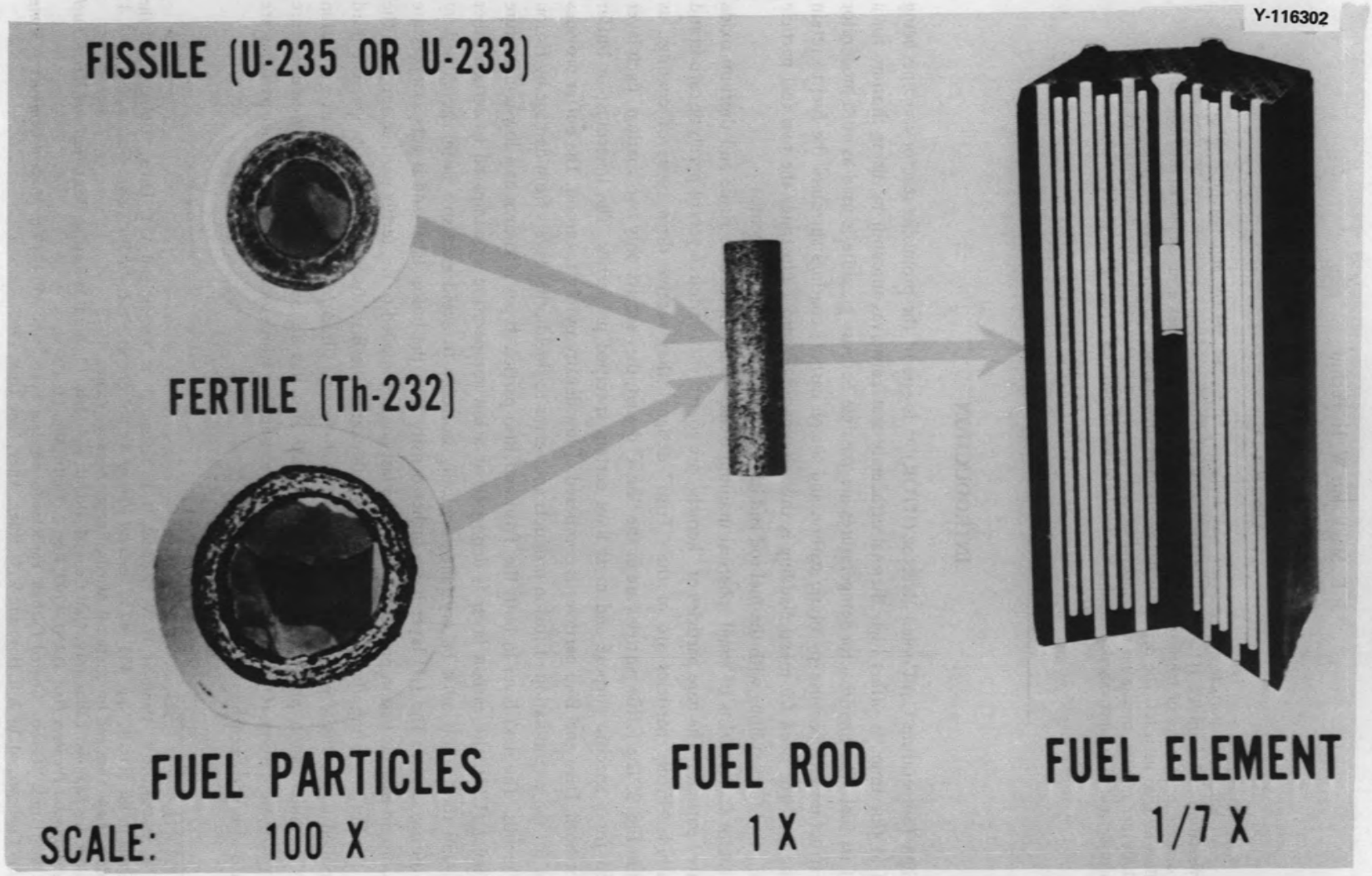

Fig. 1. HTGR fuel components.

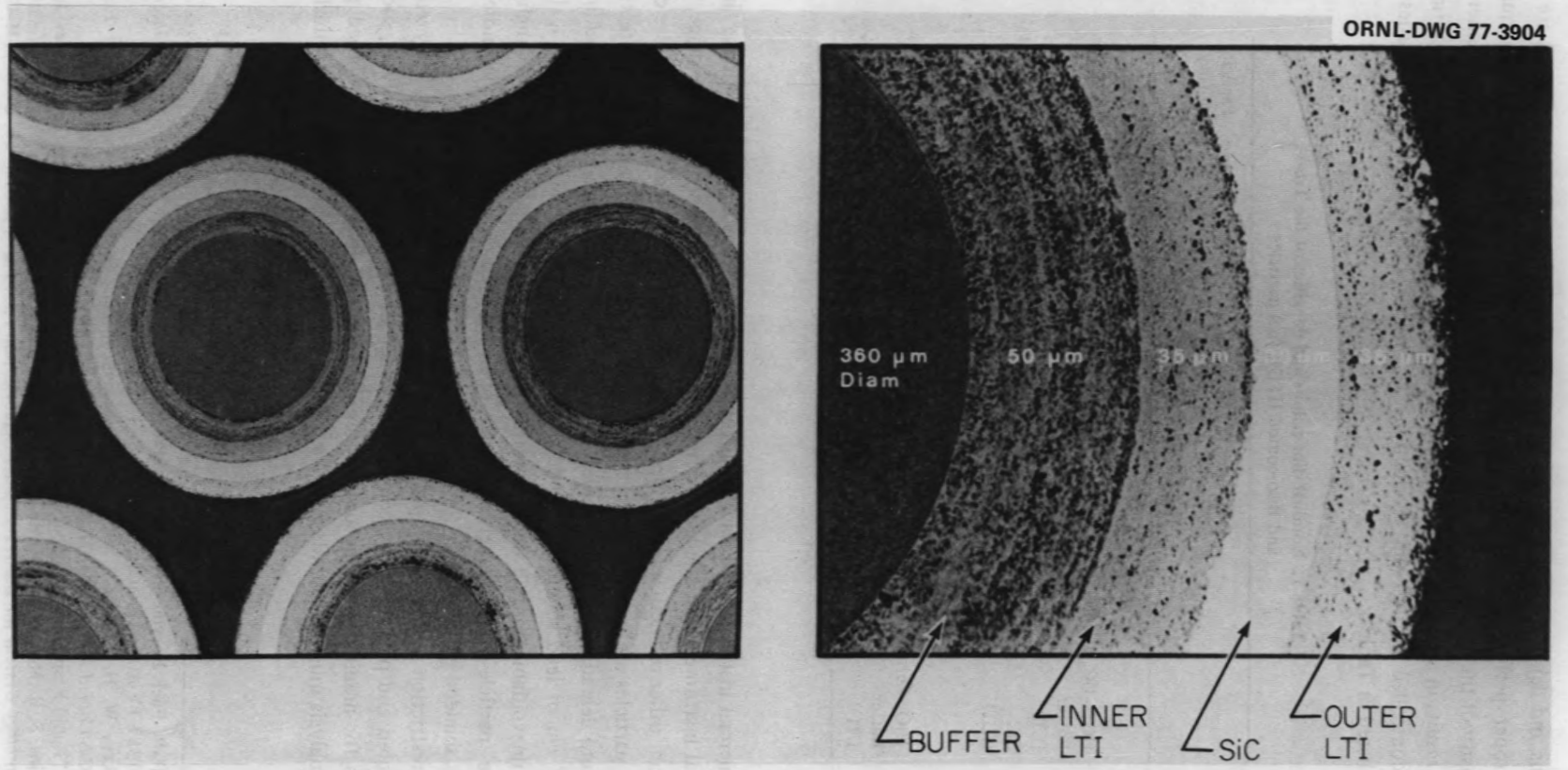

Fig. 2. HTGR "Triso" design fissile fuel particles.

The dimensions and densities of the kernels and coating layers in HTGR fuel particles are properties of prime interest. Proper performance of the intended function of each coating layer requires that the thickness and density of the applied coating material be within a specified range.[4] The manner in which the coating is applied results in a variation in coating thickness from particle to particle.[5] This variation must be determined and controlled during fuel production. The nominal dimensions and densities for the two particle types are listed in Table 1.

Table 1. Nominal dimensions and densities of the Triso- and Biso-coated HTGR fuel particles

	Coating thickness (μm)	Coating density (kg/m^3)	Particle diameter (μm)	Particle density (kg/m^3)
		Fissile (Triso)		
UO_2-UC_2 kernel			400	3.2×10^3
Buffer	50	1.1×10^3	500	2.2×10^3
ILTI	35	1.9×10^3	570	2.1×10^3
SiC	30	3.2×10^3	630	2.4×10^3
OLTI	35	1.9×10^3	700	2.3×10^3
		Fertile (Biso)		
ThO_2 kernel			500	10.0×10^3
Buffer	85	1.1×10^3	670	4.8×10^3
LTI	75	1.9×10^3	820	3.5×10^3

Several commercial instruments are available for measuring and/or counting particles;[6] however, none of the commercial instruments satisfied our criteria. Besides our requirements for size range, precision, and speed of operation, other restrictions were imposed on a measuring device due to the nature of the material in question. The particles are pyrophoric at several stages, requiring inert atmosphere protection to prevent rapid oxidation and degradation. Also, samples containing as little as one-half gram of uranium will require a minimum of 5 cm of lead shielding to reduce operator exposure to acceptable limits, since the ^{233}U recycle fuel will unavoidably contain trace quantities of ^{232}U along with its associated daughter products.[7] Accordingly, the particle-size analyzer must be operated and maintained semiremotely within an inert-atmosphere, shielded glove box.

One further restriction is that of sample reclamation. Once the sample has been analyzed and weighed, it must be collected and pneumatically conveyed to other stations for further analyses, such as impurity analysis; analysis for uranium, carbon, and oxygen content; and inspection for damaged particles. As a result, the size analysis must be a nondestructive technique, and damage to the particles must be absolutely minimized.

4. ORNL HTGR Fuel Recycle Development Program, *Interim I HTGR Recycle Fuel Product Specifications,* Document No. D-11387-TV-A01-0, January 31, 1975.

5. W. J. Lackey, W. H. Pechin, J. D. Sease, *Measurement and Control of the Shape of Fuel Particles for High-Temperature Gas-Cooled Reactors,* ORNL/TM-4673 (Nov. 1974).

6. R. Davies, "Rapid Response Instrumentation for Particle Size Analysis," American Laboratories, Jan. 1974.

7. J. D. Jenkins, S. R. McNeany, J. E. Rushton, *Conceptual Design of the Special Nuclear Material Nondestructive Assay and Accountability System for the HTGR Fuel Refabrication Pilot Plant,* pp. 27–58, ORNL/TM-4917 (July 1975).

RADIOGRAPHIC TECHNIQUE FOR THE MEASUREMENT OF COATING THICKNESS

One way in which the particle diameter and the thicknesses of the various coatings have been measured in the past is by microscopic examination of an x-radiograph[8] of the particle sample. This method has been routinely employed since the early stages of microsphere coating development in the HTGR Fuel Refabrication Program. With this method, a batch need not be sampled until the final coating has been applied, since radiography reveals the inner structure of the particle and thus permits thickness measurements to be made on each coating.

The equipment used to read the radiographs is shown in Fig. 3. It consists of a microscope with a filar eyepiece (which is calibrated using a calibration slide), a PDP-8/E (Digital Equipment Corporation) computer to perform the calculations, and a teletype to provide printout. Once the computer is ready to accept data, the operator aligns the hairline in the eyepiece with the outer edge of the particle or at a coating interface, depending on which information is required. The position of the hairline shown on the microcode display is entered into the computer when the operator presses the "read" button.

8. R. W. McClung, *Studies in Contact Microradiography,* ORNL/TM-3511 (October 1963).

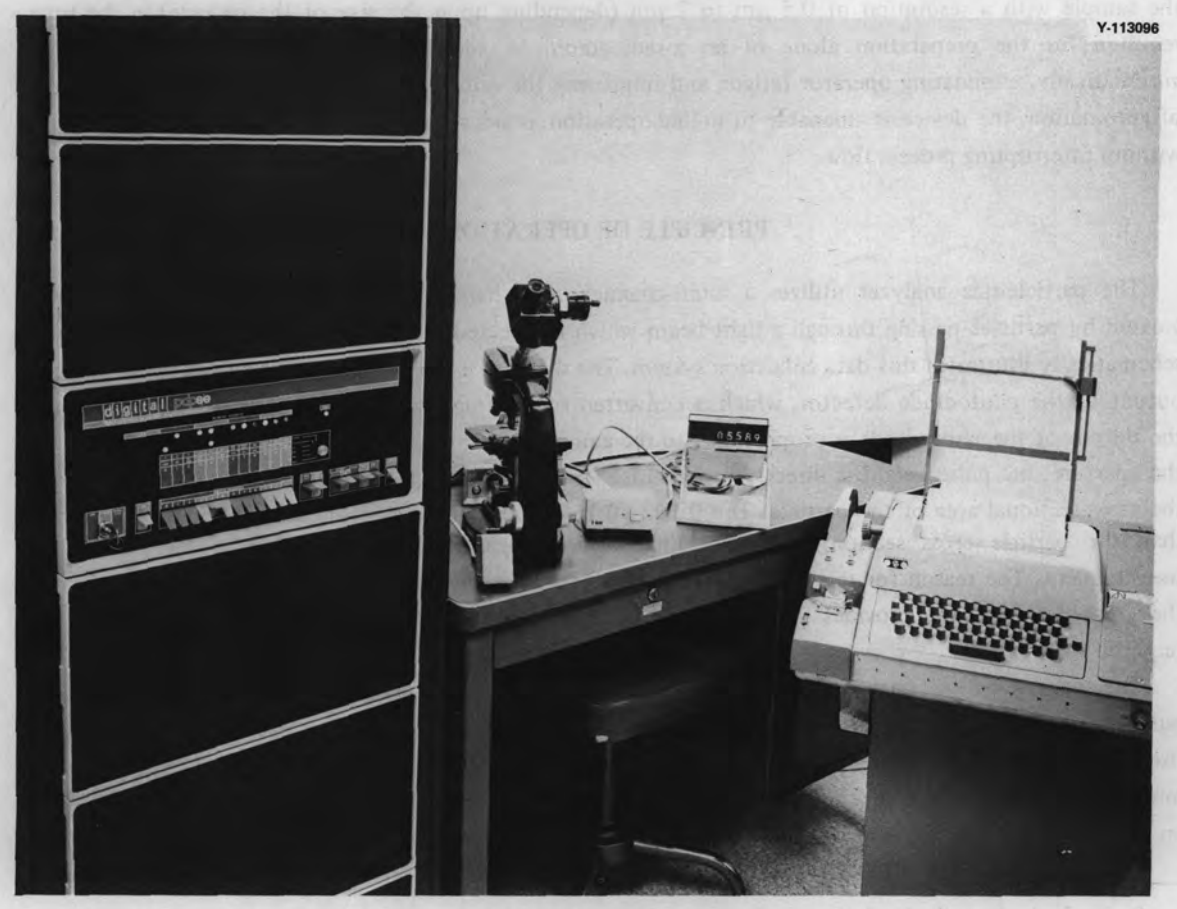

Fig. 3. Equipment used to read particle size and coating thickness from an x-radiograph of the sample.

As many as ten readings may be taken on a single Triso-coated particle to determine particle and kernel diameters, as well as the thickness of each coating. A shape ratio is obtained from these readings by comparing the coating thickness on one side to that on the other; this provides a measure of sphericity. A spherical particle will have a shape ratio of 1.00, while a multifaceted particle will have a shape ratio as high as 1.30.[9] The more faceted a particle is, the greater the number of stress points in the coating and the higher the probability of failure during irradiation.[10] Rotation of the eyepiece through 360° permits several diameter and coating thickness measurements to be taken about a single particle, allowing a study of variation in coating thickness within individual particles. Together with the information on particle-to-particle variation, this provides a physical basis for evaluating and modifying the coating process.

The radiograph has a resolution of about 1 μm, which is adequate. However, to determine the variation from particle to particle and to adequately determine the mean dimension, it is necessary to measure 30 to 50 particles and calculate the mean and standard deviation of the individual measurements. For diameter measurements on 50 particles, the 95% confidence interval about the mean diameter is typically ±3 to 6 μm. With manual recording and calculation of the data, this operation requires several hours. Automatic data acquisition reduces the time for measurements and calculations to 15 to 20 min, but the preparation of the radiograph remains a relatively lengthy process, and operator fatigue limits the rate at which radiographs can be read.

In order to eliminate the disadvantages inherent in this technique, an automated particle-size analyzer has been developed. The design of the device is such that it permits rapid measurement of each particle in the sample with a resolution of 0.5 μm to 2 μm (depending upon the size of the particle) in the time required for the preparation alone of an x-radiograph. In addition, the measurement is performed automatically, eliminating operator fatigue and improving the reliability of the data. Because of the degree of automation, the device is amenable to in-line operation, nondestructively providing quality control data without interrupting process flow.

PRINCIPLE OF OPERATION

The particle-size analyzer utilizes a multi-channel pulse height analyzer to measure voltage pulses created by particles passing through a light beam which is directed onto a Schottky photodiode. Figure 4 schematically illustrates this data collection system. The shadow of the particle causes a drop in the current output of the photodiode detector, which is converted to a voltage gain by an amplifier/converter. Since the output of the photodiode is proportional to the amount of light reaching the active surface exposed by the aperture, the pulse height is directly proportional to the shadow cast by the particle and therefore to the cross-sectional area of the particle. The 0.16 × 0.16 cm aperture was deliberately chosen to be larger than the particle cross section, thus providing an area measurement rather than a major diameter measurement. The reason for this is that the particles are not perfectly spherical, and the measurement of the cross-sectional area provides a compromise between the diameter and volume, both of which are required.

The spacing and velocity of the particles through the light beam must be such as to provide the proper pulse shape for the electronics. The particles must travel through the light beam fast enough to present a rise time short enough to peak within the electronic gate of the analog-to-digital converter (125 μsec). They must also pass through the light beam individually, since the appearance of more than one particle shadow on the detector at a given time will result in an error in both particle size and count. To prevent this, the

9. W. L. Lackey, W. H. Pechin, J. D. Sease, *Measurement and Control of the Shape of Fuel Particles for High-Temperature Gas-Cooled Reactors,* ORNL/TM-4673 (Nov. 1974), p. 5.

10. W. J. Lackey, W. H. Pechin, J. D. Sease, *Measurement and Control of the Shape of Fuel Particles for High-Temperature Gas-Cooled Reactors,* ORNL/TM-4673 (Nov. 1974), p. 2.

ORNL-DWG 77-11781

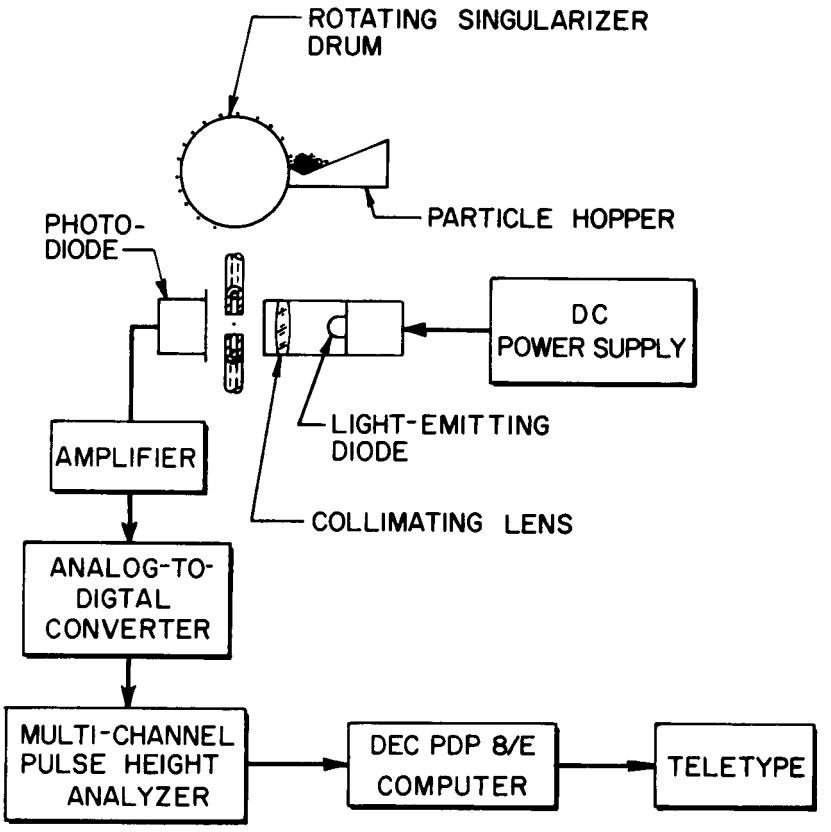

Fig. 4. Electronic particle-size analyzer (information flow diagram).

particles are picked up individually by a rotating singularizer drum, which ensures adequate spacing between particles. Their velocity is determined by the speed of the conveying air which is drawn past the detector and exhausted through a vacuum pump. A cyclone collector is used to disentrain the particles from the air stream.

To eliminate sizing discrepancies caused by different particle trajectories past the detector, the light source must provide a beam of uniform intensity across the field of the sensor. The intensity of the beam must also remain relatively invariant with time. The light source employed is a Fairchild FLV-104 light-emitting diode (LED) with a rated output of 100 mcd operating in the near-red region. The LED is driven by a 6-V regulated dc power supply. Uniformity of the beam is achieved by locating the LED at the focal point of a plano-convex lens, producing a beam of parallel light by essentially focusing the LED at infinity.

The instrument is calibrated with a high-precision (AFBMA Grade 10) calibration sample which consists of stainless steel microspheres of six sizes, ranging from 380 to 800 μm with a standard deviation of ± 1 μm at each size. Periodic checks on calibration are performed with a calibration disk built into the detection module. A separate device permits a single particle to be recirculated through the system to provide data on the precision of the instrument. Each of these techniques is discussed in detail in the following sections.

INSTRUMENT DESIGN

The particle-size analyzer is illustrated in Fig. 5. The particle sample is introduced into the singularizer hopper. Particles are transferred from the hopper to the delivery tube by means of the rotating singularizer drum. The drum has forty holes of 0.25-mm (0.010-in.) diameter electro-discharge machined around its circumference in a vertical plane centered with respect to the feed hopper. A vacuum inside the drum causes particles to adhere to the holes of the drum as it rotates past the feed hopper. A Teflon nozzle located inside the drum (not shown) provides an air jet which blows the particles off the drum toward the delivery tube. A doublet blow-off jet located above the drum removes any particles not seated in a drum hole, as some particles may cling to the primary particle due to static charge. A photograph of the singularizer is presented in Fig. 6.

A second vacuum pump is used to draw the particles into the delivery tube, through the light beam in front of the detector, and into a cyclone receiver. The particles enter the cyclone receiver tangentially so as to minimize damage to the coatings, and they gradually lose their velocity in the outer slow-speed vortex. The particles are disentrained from the air stream at this point, and are collected in the sample bottle. A rotating vacuum lock has been designed, fabricated, and tested which dispenses the sample to an analytical balance to obtain the sample weight without disrupting the vacuum inside the cyclone receiver.

Particles are fed through the analyzer at rates of 500 to 2000 particles per minute. A stepping motor and indexer control the drum speed and consequently the particle feed rate. Use of the indexer permits the counting out of a specified number of particles; the drum can be stopped after a certain number of steps have been executed. A positive acting gear pulley and toothed drive belt eliminate slippage and increase the precision of the drum setting.

As the particles pass in front of the Schottky photodiode, the current output signal from the detector decreases momentarily by an amount exactly proportional to the cross-sectional area of the particle. The detector output is fed to the amplifier/converter, which converts the milliamp drop to a millivolt gain and amplifies and shapes it to obtain a voltage pulse from 0 to 4 V, depending on the size of the particle. This signal is fed to an analog-to-digital converter which determines the maximum peak height of each pulse by digitizing the pulse when the sign of the derivative changes. This value is then stored as a single count in one of 1024 channels of the multi-channel pulse height analyzer. The channels are linear with respect to voltage, providing a resolution of $\sim$4 mV per channel. Since the particle's cross-sectional area is proportional to the voltage, the area is also linear with respect to channel number, with a resolution of 1000 μm^2 per channel. Particle diameter is not linear but quadratic with respect to channel number, ranging from 2 μm per channel at the low end of the scale to 0.5 μm per channel for large particles.

To determine the precision of the instrument, a single particle repeater was designed and fabricated to permit recirculation of a single particle through the particle-size analyzer. The repeater was based on a rotating vacuum lock scheme, consisting of a drum containing six pockets and a Teflon vacuum seal. The device is attached to the outlet of the cyclone receiver and both are then positioned above the singularizer hopper. This arrangement is illustrated in Fig. 7. One or more particles are introduced into the system by being dropped into the singularizer hopper. Each time the particle passes through the analyzer, a measurement is recorded. The particle is then disentrained from the air stream in the cyclone receiver and falls into one of the pockets in the rotating repeater drum. The particle is removed from the vacuum and dropped into the singularizer hopper for the next measurement. This recycling continues until $\sim$200 counts have been accumulated. Each cycle requires 3 to 5 sec for completion. By running particles of several different sizes simultaneously, an entire spectrum can be accumulated in 15 min.

Using the single particle repeater, steel microspheres of diameter 600 μm and larger indicated standard deviations on the order of $\pm$1 μm for repeated measurements of the same particle. For steel microspheres of

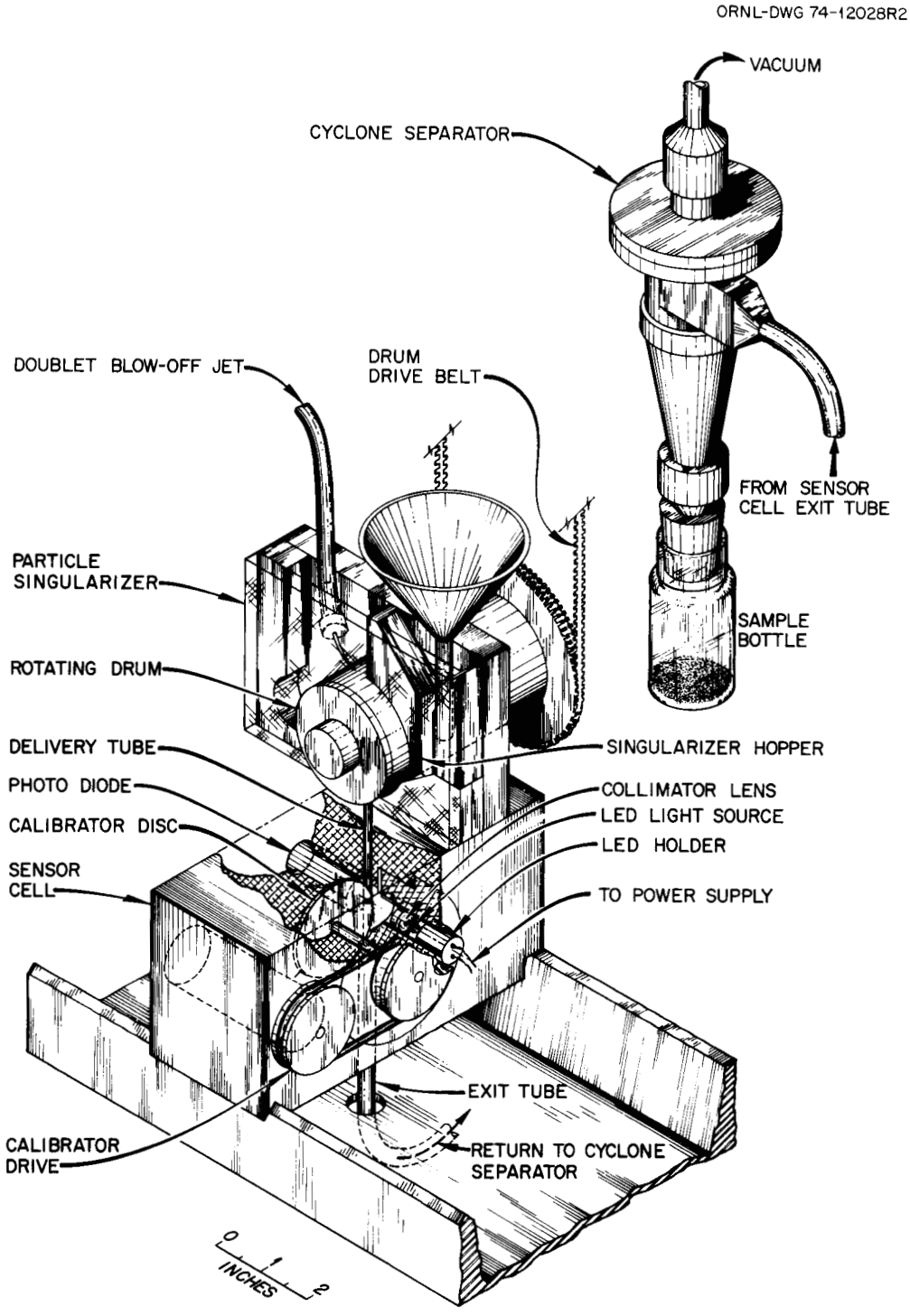

Fig. 5. Particle-size analyzer.

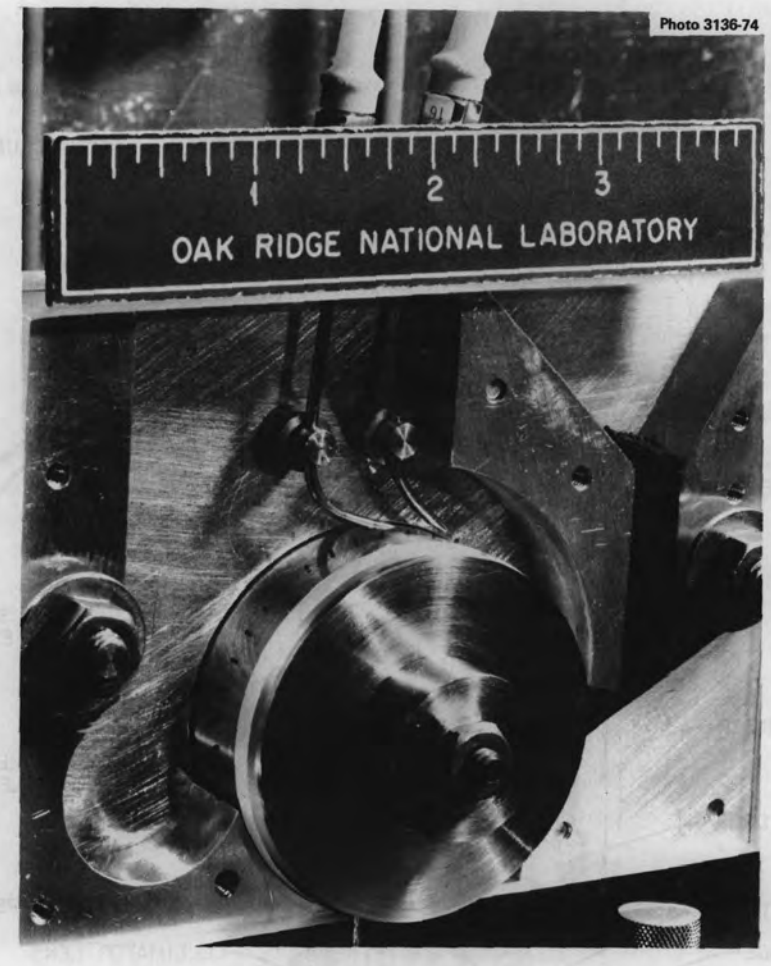

Fig. 6. The singularizer drum and hopper of the particle-size analyzer.

375 μm diameter, the standard deviation was on the order of ±2 μm. By repeatedly measuring the same spherical particle and accumulating a spectrum, we were able to assess the intrinsic precision and accuracy of the particle-size analyzer.

Repeated measurement of individual fuel particles produces a much broader distribution than for the steel microspheres, because the fuel particles are less spherical. The indicated size of the fuel particle depends on which cross-sectional view it presents as it passes in front of the detector. Recirculating three coated particles of ∿650 μm diameter produced distributions with standard deviations of 5.2, 5.4, and 7.8 μm, increasing with the individual particle shape ratios which had been measured prior to sizing – the largest of these being 1.26. Since a typical sample contains 5000 to 10,000 particles, the variance due to particle shape in the individual measurements does not appreciably affect the determination of the mean diameter of the sample, as evidenced by the close agreement in mean diameter when the same sample is sized repeatedly. Also, since the standard deviations of the samples are typically ±20 to 40 μm due to the random nature of the coating process, the variance in individual measurements represents only a slight contribution to the overall standard deviation.

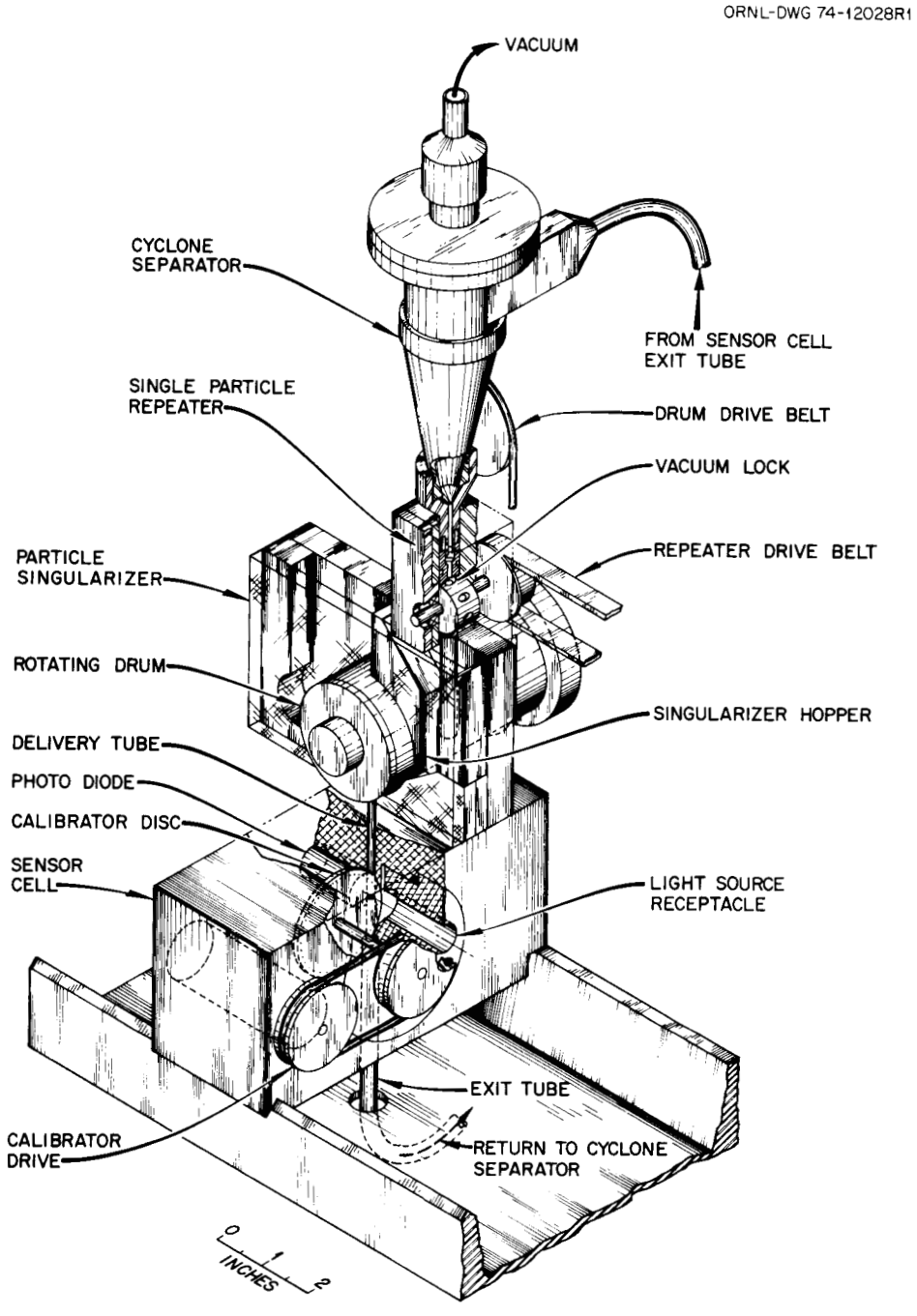

Fig. 7. The particle-size analyzer with single particle repeater.

INSTRUMENT CALIBRATION

As mentioned earlier, the magnitude of the voltage pulse created by the particle is directly proportional to the cross-sectional area of the particle. Calibration of the particle-size analyzer is then based on the linear voltage-to-area relationship $y = ma + b$, where y is the channel number registering the count, a is the cross-sectional area of the particle, and m and b are constants which must be determined. The primary calibration standard for the analyzer consists of a set of high-precision stainless steel microspheres of four sizes, ranging from 380 to 800 μm, with 200 to 300 microspheres per size. Within each size range there is a size variation of ±1.25 μm (±0.000050 in.) as provided by the manufacturer.

The calibration sample produces four distinct peaks across the spectrum of the analyzer. The mean channel of each distribution is calculated according to the formula:

$$I_N = \frac{\sum_{i=j}^{j+n} i \cdot C_i}{C_N} , \tag{1}$$

where I_N is the mean channel of the Nth distribution which registers counts in n channels beginning in channel j. C_i is the number of counts registering in channel i, while C_N is the total number of counts in the Nth distribution.

Accordingly, four mean channels are calculated and stored in the memory of the computer. The cross-sectional area of each of the four sizes of microspheres is calculated, based on the known diameters, and a least squares fit is performed to determine the slope m (in channels/μm^2) and the intercept b (in terms of channels) of the calibration equation. Fig. 8 illustrates the relationship between cross-sectional areas, diameter, and channel number based upon this calibration. The m and b values are then stored for

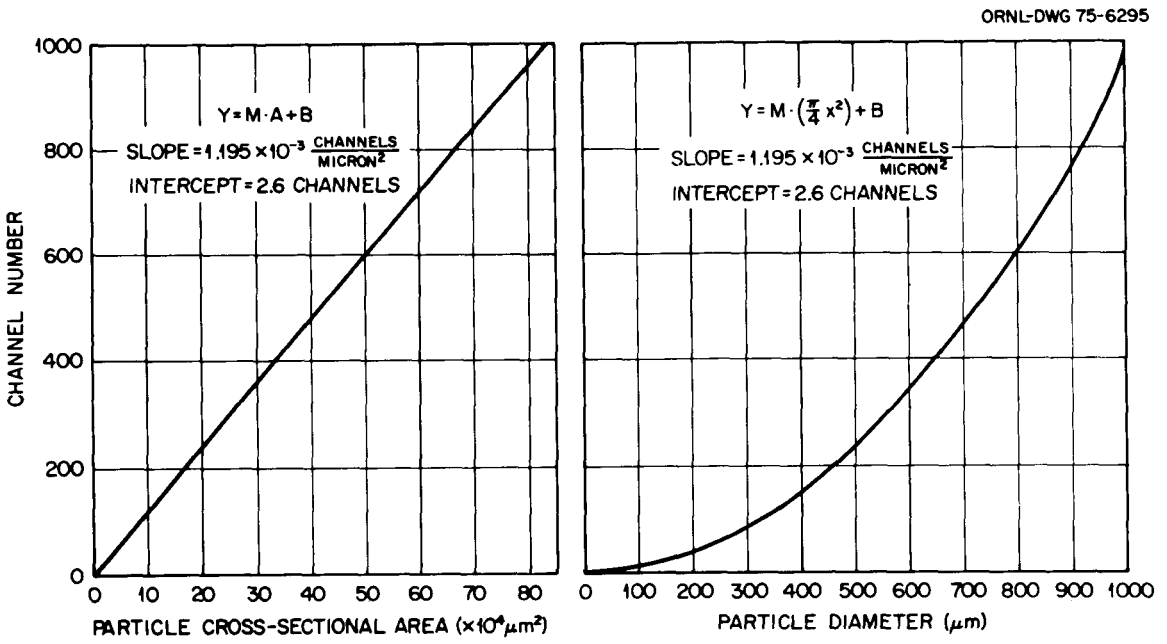

Fig. 8. Calibration curve based on the steel microsphere calibration set, plotting channel number as a function of cross-sectional area and of particle diameter.

later use with sample runs. This procedure, which requires ∿5 min to complete, is performed as indicated by the secondary calibration technique described below.

Immediately following the primary calibration, a calibration disk contained within the detection module is rotated at 6000 rpm for 10 sec and a spectrum is accumulated. The disk consists of a plexiglass hub to which six wires are attached radially at 60° intervals. The wires protrude into the light beam in front of the photodiode while the disk is spinning, as illustrated in Fig. 9, creating pulses similar to those of the particles. The "effective spherical diameter" of each wire is then determined according to the location of its mean channel on the primary calibration curve.

The disk is run prior to each sample as a secondary standard to ensure the validity of the calibration curve. Any drift caused by slight alteration in alignment or intensity of the light-emitting diode, changes in temperature, or aging of the electronic components is detected by changes in the "effective spherical diameters" of the wires. If the indicated diameter of the largest-sized wire (∿1000 μm) varies by more than 0.5 μm from the expected value, the analyzer is recalibrated using the effective diameters determined at the time of primary calibration and the current mean channels. Subsequent particle samples are then measured according to this secondary calibration curve. Should the indicated diameter of the largest-sized wire vary by more than 2 μm from its value at primary calibration, the instrument is recalibrated with the primary calibration set.

Once the mean channel of a particle sample distribution has been determined, the variance of the distribution is then calculated according to the relationship:

$$\sigma_N^2 = \frac{\sum_{i=j}^{j+n} (I_N - i)^2 \, C_i}{C_N} , \qquad (2)$$

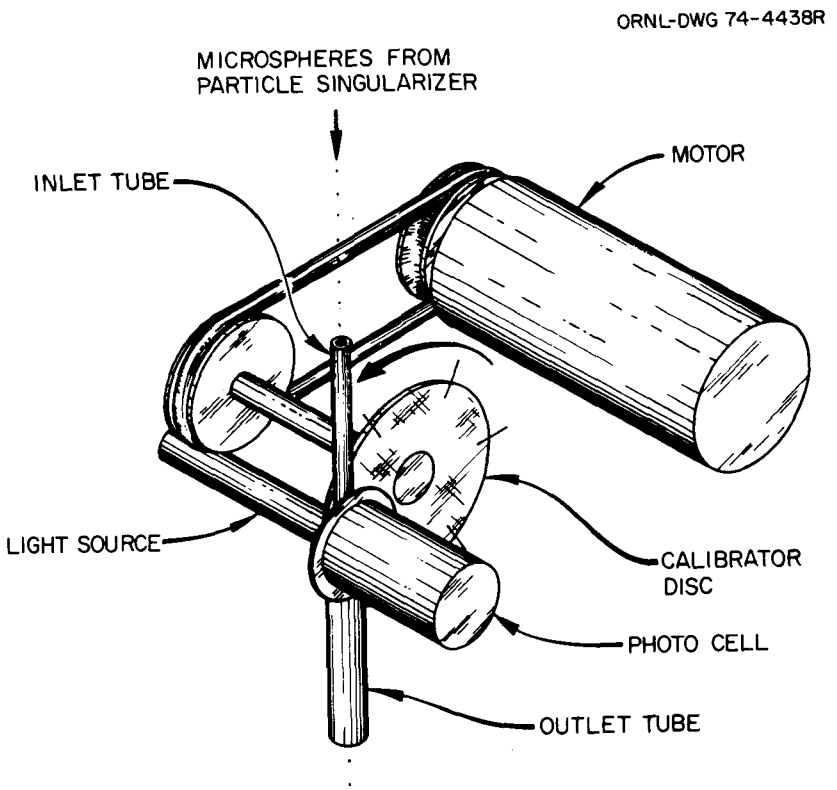

Fig. 9. The wire disc as a secondary calibration standard for the particle-size analyzer.

where σ_N is the standard deviation of the Nth distribution in terms of channels, the variance being the square of the standard deviation. The standard deviation of the area measurements, σ_a, is given by σ_N/m, where m is the slope of the calibration curve. The standard deviation of the diameter measurements, σ_d, can be calculated from the relation:

$$\frac{\sigma_a}{a} = \frac{2\sigma_d}{d} , \tag{3}$$

where a is the mean particle area and d is its corresponding diameter. This value of σ_d is a measure of the sample spread.

It should be noted here that while d is easily calculated, it is not, strictly speaking, the mean particle diameter. The mean area, $\overline{A}$, of a given normal distribution of diameters is given by:[11]

$$\overline{A} = \frac{\pi}{4}(\overline{D}^2 + \sigma_D{}^2) , \tag{4}$$

where $\overline{D}$ is the mean diameter and $\sigma_D{}^2$ is the variance of the particle diameter distribution. In a similar manner, the mean volume is given by:

$$\overline{V} = \frac{\pi}{6}(\overline{D}^3 + \sigma_D{}^2 \cdot \overline{D}) . \tag{5}$$

For a normal diameter distribution, the area and volume distributions will be skewed to the left, the amount of skewness depending on the variance of the diameter distribution.

By calculating a diameter from the mean area, we are essentially taking the "middle" value, minimizing errors in using this value in coating thickness or volume calculations. This approach is taken solely because of current computer programming limitations. The errors introduced in making such a measurement are given in terms of the diameter and variance as follows:

$$\overline{A} = \frac{\pi}{4} \widetilde{D}^2 , \tag{6}$$

where $\widetilde{D}$ is the diameter corresponding to the mean area.

Then

$$\overline{D} = \sqrt{\widetilde{D}^2 - \sigma_D{}^2} \tag{7}$$

$$\frac{\overline{D}}{\widetilde{D}} = \sqrt{\frac{\widetilde{D}^2 - \sigma_D{}^2}{\widetilde{D}^2}} \tag{8}$$

and

$$\frac{\overline{D}}{\widetilde{D}} = \sqrt{1 - \frac{\sigma_D{}^2}{\widetilde{D}^2}} . \tag{9}$$

11. Personal communication, C. K. Bayne, Mathematics Research Dept., UCC-ND (Y-12), December 1976.

Also,

$$\tilde{V} = \frac{\pi}{6} \tilde{D}^3 \tag{10}$$

and

$$\tilde{V} = \frac{\pi}{6} (D^2 + \sigma_D{}^2)^{3/2} \ . \tag{11}$$

Then

$$\frac{\bar{V}}{\tilde{V}} = \frac{(\bar{D}^3 + 3\sigma_D{}^2 \bar{D})}{(\tilde{D}^2 + \sigma_D{}^2)^{3/2}} \ . \tag{12}$$

The calculated diameter is slightly larger than the true mean, while the calculated volume is slightly lower.

For most particle samples, σ_D varies between 20 and 40 μm, while particle diameters range from 400 to 850 μm. For a typical sample with a particle diameter of 600 μm and a standard deviation of 30 μm, the diameter ratio from Eq. 9 is 99.875%, while the volume decrease from Eq. 12 is on the order of 0.37%. This effect increases for smaller diameters and larger variances. For calibration purposes, this effect can be neglected due to the small variance of the peaks ($\sigma \cong 2.0$ μm) and the relatively large particle diameters (400 to 800 μm).

CALIBRATION ACCURACY

In calibrating the analyzer, the uncertainty in the sizes of the steel microspheres and their peak channels gives rise to an error term to be included with the particle sample's standard deviation. Once the mean channel of a distribution (y) has been determined, the mean cross-sectional area is determined according to the relationship:

$$\bar{a} = \frac{1}{m} (\bar{y} - b) \ . \tag{13}$$

The particle sample diameter d is then calculated from $\bar{a}$. The variation in $\bar{a}$ due to the deviation in $m, \bar{y}$, and b is given by:

$$\sigma_{\bar{a}}{}^2 = \bar{a}^2 \left[\frac{\sigma_{\bar{y}}{}^2 + \sigma_b{}^2}{(\bar{y} - b)^2} + \frac{\sigma_m{}^2}{m^2} \right] \ . \tag{14}$$

While $\sigma_{\bar{y}}$ can be calculated directly from the spectrum, the variation in m and b must be calculated beforehand.

The slope is calculated according to the least squares fit equation:

$$m = \frac{n \sum_{i=1}^{n} a_i y_i - \sum_{i=1}^{n} a_i \sum_{i=1}^{n} y_i}{n \sum_{i=1}^{n} a_i{}^2 - \left(\sum_{i=1}^{n} a_i \right)^2} , \tag{15}$$

for a calibration set consisting of n sizes of steel microspheres where a_i is the cross-sectional area of the ith size of steel microspheres and y_i is its peak channel as recorded by the analyzer. The variance in m will then be the sum of the weighted variances in the a_i and y_i measurements. Accordingly,

$$\sigma_m{}^2 = \sum_{i=1}^{n} \left(\frac{\partial m}{\partial a_i}\right) \sigma_{a_i}{}^2 + \sum_{i=1}^{n} \left(\frac{\partial m}{\partial y_i}\right)^2 \sigma_{y_i}^2 = \sigma_m{}^2(a) + \sigma_m{}^2(y) \,. \tag{16}$$

The variance in a_i corresponds to the error in measuring the diameters x_i of the calibration microspheres. The variance in the peak channels y_i can be calculated directly from the channel/count distribution.

Evaluating the partial derivatives we get:

$$\sigma_m^2\,(a) = \frac{\sum_{j=1}^{n} \left\{ 2\left(na_j - \sum_{i=1}^{n} a_i\right)\left(n\sum_{i=1}^{n} a_i y_i - \sum_{i=1}^{n} a_i \sum_{i=1}^{n} y_i\right) - \left(ny_j - \sum_{i=1}^{n} y_i\right)\left[n\sum_{i=1}^{n} a_i^2 - \left(\sum_{i=1}^{n} a_i\right)^2\right]\right\}^2 \sigma_{a_j}^2}{\left[n\sum_{i=1}^{n} a_i^2 - \left(\sum_{i=1}^{n} a_i\right)^2\right]^4} \tag{17}$$

and

$$\sigma_m^2(y) = \frac{\left[\sum_{j=1}^{n} \left(na_j - \sum_{i=1}^{n} a_i\right)^2 \sigma_{yj}^2\right]}{\left[n\sum_{i=1}^{n} a_i^2 - \left(\sum_{i=1}^{n} a_i\right)^2\right]^2} \,. \tag{18}$$

Once we have calculated m we can obtain b from the relation:

$$b = y^* - ma^* \,, \tag{19}$$

where

$$y^* = \frac{1}{n}\sum_{i=1}^{n} y_i \tag{20}$$

and

$$a^* = \frac{1}{n}\sum_{i=1}^{n} a_i \,. \tag{21}$$

The variance in b is then given by:

$$\sigma_b^2 = \sigma_{y*}^2 + m^2 \sigma_{a*}^2 + a^{*2} \sigma_m^2 \,, \tag{22}$$

where

$$\sigma_{y*}^2 = \frac{1}{n^2} \sum_{i=1}^{n} \sigma_{y_i}{}^2 \tag{23}$$

and

$$\sigma_{a*}^2 = \frac{1}{n^2} \sum_{i=1}^{n} a_i{}^2 \,. \tag{24}$$

The variation can then be rewritten as:

$$\sigma_b^2 = \frac{1}{n^2} \left[\sum_{i=1}^{n} \left(\sigma_{y_i}{}^2 + m^2 \sigma_{a_i}{}^2 \right) + \left(\sum_{i=1}^{n} a_i \right)^2 \sigma_m{}^2 \right] . \tag{25}$$

Table 2 lists the results of light-wave micrometer measurements of the steel microsphere calibration sample. One percent of the microspheres were sized in this manner. Traceability to the National Bureau of Standards was established through ORNL secondary standards set no. UCC 72, serial no. 7.1669 CRAA5, calibrated February 25, 1976.

The analyzer's measurement of the peak channels for the calibration sample yields standard deviations ranging from 1.00 to 1.30 channels. Using these values for the σ_{y_i} together with the σ_{a_i} from Table 2, the uncertainty in the mean diameter at the 95% confidence level due to calibration error was calculated to be less than ±0.30 μm.

The calculated curve fits the particle size within the total 95% confidence interval for the larger-sized particles. At the low end, the calculated value is still within 0.3 or 0.4 μm, although the fit to the curve is not as good. R-square values of 0.9999 are typical.

Since we are dealing with coated particle samples containing several thousand particles and standard deviations ranging from 20 to 40 μm, the error introduced in calibration is minimal, as is the effect of variance from the curve for smaller-sized particles.

Table 2. Measurement of steel microsphere calibration sample by light-wave micrometer

Mean diameter (μm)	Standard deviation (μm)	95% confidence interval (μm)
379.16	0.21	0.11
506.15	0.34	0.18
633.10	0.17	0.09
791.99	0.17	0.09

DATA ACQUISITION

As discussed earlier, the current output of the photodiode is fed to an amplifier/converter which converts current drops into positive voltage pulses which are digitized by an analog-to-digital converter (ADC) and stored in a multi-channel analyzer. The multi-channel pulse height analyzer (Nuclear Data 2400 model) has a 100-Mhz ADC with a conversion gain selectable from 256 to 8192 channels for an 8-V full-scale signal. The analyzer typically operates with a conversion gain of 4096, providing a scale of 0 to 4 V which may be selected and expanded for viewing. The memory section is capable of recording 1024 channels with a full-scale zero suppression, allowing the recording of any 1024-channel segment of the output even at the highest conversion gain. It also has the capability of being broken down into as many as four equal portions of 256 channels each, with the ability to accumulate an individual spectrum in each portion. Control over these functions provides great flexibility in accumulating spectra of the steel microspheres, calibration disk, and fuel particle samples.

Figure 10 is a photograph of the particle-size analyzer set to recirculate a single particle or several particles of different sizes. At the upper right are the pressure gauges which indicate singularizer drum vacuum, blow-off jet pressure, and transfer vacuum. Directly below these is located the cyclone receiver, which receives particles from the detection module through the polyethylene tubing entering from the right. Attached to the bottom of the receiver is the rotating vacuum lock which collects the disentrained particle and drops it into the singularizer hopper. Located under the singularizer drum, the detection

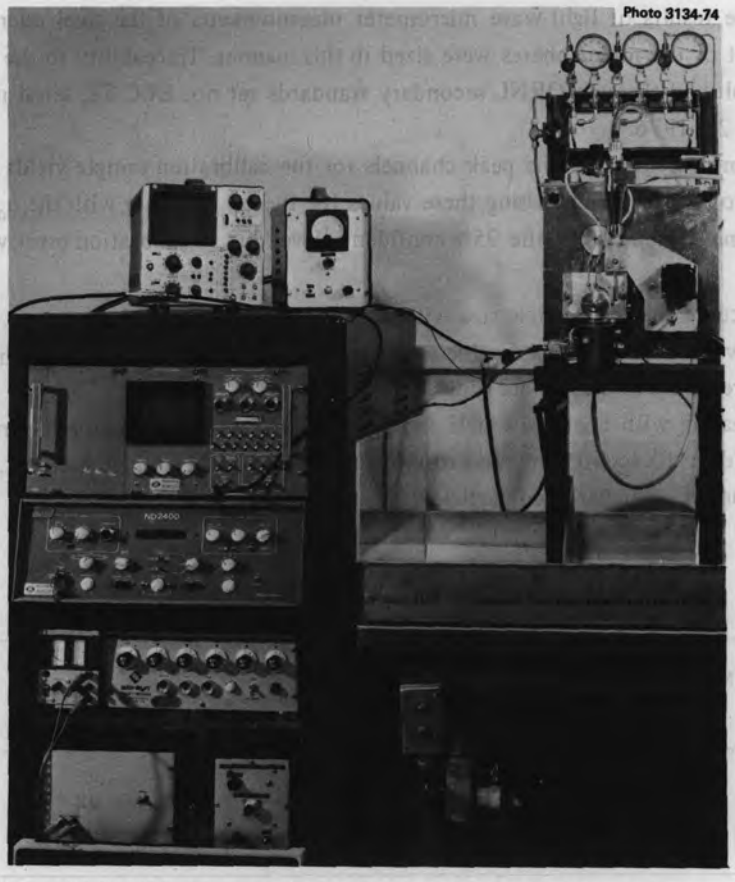

Fig. 10. Particle-size analyzer with single particle repeater and data collection system, excluding computer and teletype.

module houses the light source, sensor, and calibration disk. On the left are an oscilloscope and the amplifier/converter on top of the rack. Below these are the multi-channel pulse height analyzer, indexer for the singularizer drum, and the regulated power supply and controls for the calibration disk.

After a spectrum has been accumulated, the data is transferred automatically from the analyzer to the computer system, a PDP-8/E computer modified by the addition of a 1k read-only memory, the expansion of the original 4k core to 8k, and the addition of a Sykes Compucorder 100 magnetic tape cassette unit to permit the rapid exchange of programs. The tape cassette allows the computer to be used for several instruments in addition to the particle-size analyzer. The computer is programmed in FOCAL, an interactive language of sufficient simplicity to permit the rapid preparation and modification of programs for processing the data.

SUMMARY

To briefly summarize the operation of the particle-size analyzer, fuel particles ranging in diameter from 300 to 1000 μm are individually measured at rates up to 2000 per minute and collected undamaged for further analysis. Samples containing 5000 to 10,000 particles can be measured and weighed within 10 to 15 min, providing information on the particle-size distribution, number of particles, and sample weight. From this information can be calculated a mean particle diameter, the standard deviation of the distribution, and mean particle weight, volume, and density. By sampling both before and after the application of a coating layer, we can determine the mean thickness, volume, and density of that layer. This information can all be obtained within a turnaround time acceptable for altering or modifying the coating process to compensate for changing conditions.

Because of its size and the small number of moving parts, the particle-size analyzer is readily adaptable to remote operation and glove box maintenance. Only the singularizer, hopper, detection module, and cyclone receiver need to be located within the enclosure, occupying a space of approximately 1 ft^3. All of the control mechanisms can be located at the operator's station, together with the computational equipment and data printout. These features make the particle-size analyzer ideal for measuring spherical or near-spherical radioactive or toxic particles in a remote facility.

ACKNOWLEDGMENTS

The authors wish to thank L. J. Turner for his perseverance and contributions to the development of the particle-size analyzer. L. H. Thacker and W. R. Miller of the Instrumentation and Controls Division are to be commended for their development of the state-of-the-art amplifier/converter which is the heart of the particle-size analyzer's electronics. The comments of R. A. Bradley and A. J. Moorehead in editing this report are greatly appreciated. We would also like to thank Elizabeth Giddings for editing the manuscript and the Technical Publications personnel for preparing the document for reproduction.

The authors would also like to extend their appreciation to the International Atomic Energy Agency for choosing an excellent drawing of the particle-size analyzer made by H. R. Livesey for the cover of their proceedings on nuclear fuel quality assurance,[12] the drawing being a small portion of a fine presentation by W. J. Lackey of a paper authored by W. H. Pechin, W. J. Lackey, J. D. Sease, and W. P. Eatherly.

12. *Nuclear Fuel Quality Assurance: Proceedings of a Seminar, Oslo, 24–27 May 1976,* International Atomic Energy Agency, Vienna, 1976.

ORNL/TM-5907
Distribution
Category UC-77

INTERNAL DISTRIBUTION

1–2. Central Research Library
3. Document Reference Section
4–12. Laboratory Records Department
13. Laboratory Records, ORNL RC
14. ORNL Patent Office
15. R. K. Adams
16. P. Angelini
17. S. P. Baker
18. B. O. Barringer
19. B. J. Baxter
20. R. J. Beaver
21. R. Blumberg
22. B. J. Bolfing
23. R. J. Braatz
24. R. A. Bradley
25. A. J. Caputo
26. J. A. Carpenter
27. H. E. Cochran
28. D. A. Costanzo
29. F. C. Davis
30. J. P. Drago
31. R. G. Donnelly
32. D. A. Dyslin
33. D. E. Ferguson
34. P. A. Haas
35. C. C. Haws
36. F. E. Harrington
37. J. L. Heck
38. L. C. Hensley
39. R. E. Helms
40–42. M. R. Hill
43. R. M. Hill
44. D. R. Johnson
45. M. J. Kania
46–48. P. R. Kasten
49–54. W. J. Lackey
55. K. H. Lin
56. H. R. Livesey
57–58. A. L. Lotts
59–63. J. E. Mack
64. M. M. Martin
65. S. R. McNeany
66. K. J. Notz
67. A. R. Olsen
68. R. M. Peach
69–73. W. H. Pechin
74. M. K. Preston
75. R. H. Rainey
76. D. P. Reid
77. J. E. Rushton
78. T. F. Scanlan
79. D. C. Scott
80. J. H. Shaffer
81. R. L. Shepard
82. D. P. Stinton
83. R. R. Suchomel
84. V. J. Tennery
85. L. H. Thacker
86. S. M. Tiegs
87. T. N. Tiegs
88. D. B. Trauger
89. G. C. Wei
90. J. R. Weir
91. M. G. Willey
92. J. W. Woods
93. R. W. Balluffi (consultant)
94. P. M. Brister (consultant)
95. W. R. Hibbard, Jr. (consultant)
96. Hayne Palmour III (consultant)
97. N. E. Promisel (consultant)
98. D. F. Stein (consultant)

EXTERNAL DISTRIBUTION

99–100. ERDA DIVISION OF REACTOR NUCLEAR RESEARCH AND APPLICATIONS, Washington, DC 20545
Director

101. ERDA IDAHO OPERATIONS OFFICE, P.O. Box 2108, Idaho Falls, ID 83401
Barry Smith

102. ERDA OFFICE OF PROGRAM MANAGEMENT, RESEARCH AND SPACE PROGRAMS, P.O. Box 81325, San Diego, CA 92138
J. B. Radcliffe

103. ERDA SAN FRANCISCO OPERATIONS OFFICE, 1333 Broadway, Wells Fargo Building, Oakland, CA 94612
Manager

104–107. ERDA DIVISION OF WASTE MANAGEMENT, PRODUCTION AND PROCESSING, Washington, DC 20545
Acting Assistant Director for Reprocessing
Chief, Technology Branch
Chief, Projects Branch
Chief, Industrial Programs Branch

108–110. ERDA OAK RIDGE OPERATIONS OFFICE, P.O. Box E, Oak Ridge, TN 37830
Director, Research and Technical Support Division
Director, Reactor Division
F. E. Dearing, Reactor Division

111–291. ERDA TECHNICAL INFORMATION CENTER, P.O. Box 62, Oak Ridge, TN 37830
For distribution as shown in TID-4500 Distribution Category, UC-77 (Gas-Cooled Reactor Technology)

292–299. ERDA Exchange Agreements with Germany and Diazon Project

☆ U.S. GOVERNMENT PRINTING OFFICE: 1977-748-189/199